Sensitivity of the LHN Scheme to Non-Rain Echoes

Daniel Leuenberger[1], Andrea Rossa[2]

[1] *MeteoSwiss, Krähbühlstrasse 58, 8044 Zürich, Switzerland*
[2] *Centro Meteorologico di Teolo, ARPA Veneto, Via Marconi 55, 35037 Teolo, Italy*

1 Introduction

Radar-derived quantitative precipitation estimates (QPE) are becoming an increasingly important element in high-resolution numerical weather prediction (NWP). As such they complement conventional data like surface or upper-air observations. COSMO has chosen to use the Latent Heat Nudging (LHN) method (Jones and Macpherson, 1997; Leuenberger and Rossa, 2003; Klink and Stephan, 2005) to assimilate radar-derived QPE.

In a recent study Leuenberger (2005) systematically investigated the performance of the LHN scheme at meso-γ scale, both in an idealised setup and in the context of real cases. He found that LHN has considerable potential at the convective scale in that for an idealised supercell it successfully initialised the storm in a perfect environment and - to a lesser extent - in non-perfect environments in which low-level humidity or wind fields were altered. For the real case convective systems, a supercell and a squall line case, LHN was able to capture the salient features of the storms. Persistence of the assimilated systems in the subsequent free forecasts appeared to depend much on the instability of the environment into which the observed systems were forced.

Unlike conventional observations, radar data exhibit a highly variable quality, in that they are affected by a number of factors that limit their accuracy in estimating precipitation at the surface. In the context of assimilating radar-derived QPE in high-resolution NWP models this poses two salient questions, i.e. how is a specific assimilation scheme affected by errors in the observations, and how can such variable quality be accounted for?

This paper addresses the first question and presents a sensitivity study of the Latent Heat Nudging scheme to gross errors in the radar data, notably non-rain echoes. These include ground clutter returns and spurious signals due to anomalous propagation of the radar beam. Consideration is given to the dynamical response of the model to the continuous forcing of idealised and real signals during assimilation time, and to the performance of free forecasts started from the LHN analyses.

2 Methodology

2.1 Model and assimilation scheme

All simulations are conducted with the LM (Version 3.1) in an idealized mode. The parametrisation for grid-scale precipitation accounts for four categories of water (water vapour, cloud water, rain and snow), the mass fractions of rain water (q_r) and snow (q_s) are treated diagnostically. Vertical subgrid turbulence and the surface flux formulation are switched on, whereas cumulus parametrization, radiation and soil processes are switched off. The LHN scheme used in this study is described in Leuenberger and Rossa (2003).

All model integrations were uniformly performed on a 50×50 gridpoint domain. In the vertical, a stretched grid is employed composed of 60 levels and separated by 67 m near the ground and 2000 m near the model top at 23500 m. Above 11000 m a Rayleigh damping layer is used to absorb vertically propagating waves. In order to damp grid-scale noise, fourth-order numerical diffusion is applied. All simulations are integrated to 2 hours.

2.2 Setup of the sensitivity experiments

The basic atmospheric environment for the sensitivity experiments was chosen following Weisman and Klemp (1982) for the study of splitting supercell storms (Fig. 1a). They used a conditionally unstable thermodynamical profile and a moist, well mixed boundary layer with constant water vapour mixing ratio r with a reference value of $r = 12\,\mathrm{g/kg}$, yielding a lifting condensation level of ∼1500 m, a level of free convection of ∼1900 m, a level of neutral buoyancy of ∼10000 m and a Convective Available Potential Energy (CAPE) of ∼1200 J/kg. As a simplification for the present study the environmental wind was set to zero for most experiments. For selected experiments, the wind profile was set to exhibit a vertical shear of 20 m/s over the lowest 4000 m and constant wind aloft with no variations of the wind direction with height ($V = 0$). The lateral boundaries are relaxed towards the initial state throughout the whole simulation.

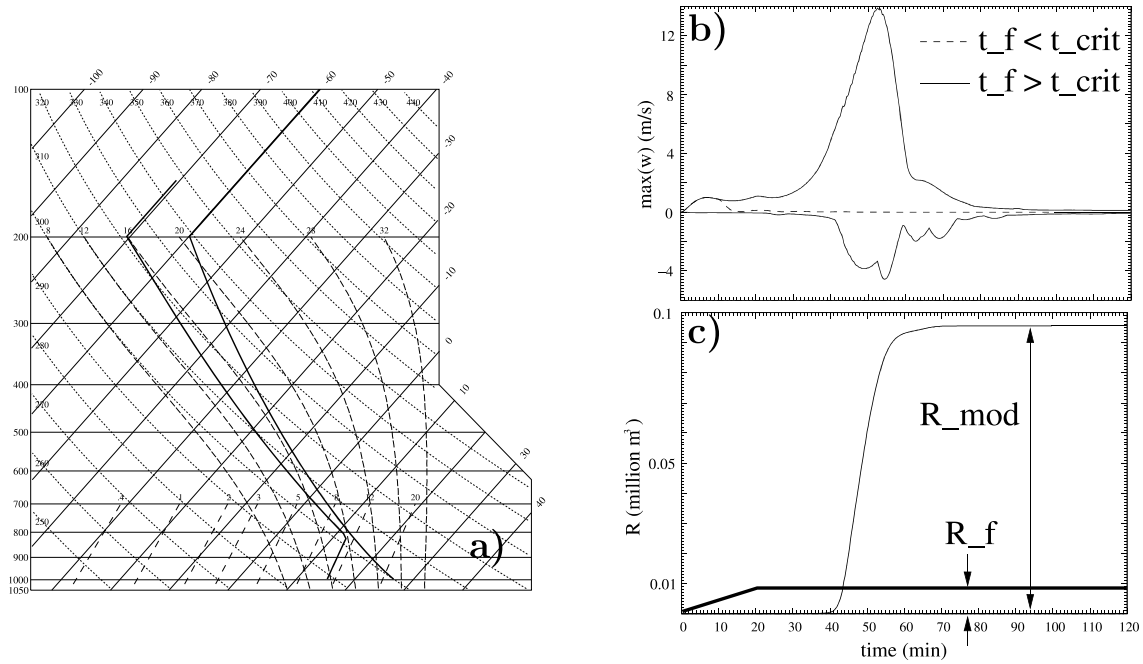

Figure 1: Panel a) shows the reference sounding following Weisman and Klemp (1982) used for the clutter experiments. The instability was varied by varying the boundary layer humidity. Here the profile for a maximum mixing ratio of 11 g/kg (resulting in a CAPE of 800 J/kg) is displayed. Panel b) displays the time evolution of the maximum up- and downdraft (m/s) during an individual assimilation and subsequent forecast experiment. The solid (dashed) line denotes an experiment in which the convective instability was (not) released (i.e. the forcing time is larger (smaller) than the critical forcing time). Panel c) shows the corresponding cumulated forcing (R_f) and resulting model precipitation (R_mod) (mm) for an experiment in which the convective instability is released with a corresponding ratio of roughly 10.

Ground clutter can be considered as one of the most important source of non-rain echoes, most of which is eliminated by appropriate clutter filters. However, in order to minimise eliminating real rain echoes, MeteoSwiss' clutter filter, for instance, leaves some 2% of the non-rain echoes in the data (Germann and Joss, 2004). This residual clutter often manifests as small-scale, quasi-static, medium to high intensity signals. On the basis of this, ground clutter is modeled for the purposes of this study as isolated, one-pixel signals of varying intensities I_f. These signals are assimilated during forcing times of various length (t_f). The boundary layer humidity was varied to obtain environments of various degrees of instability (see Tab. 1). An NWP model's numerical diffusion scheme is designed to act strongly upon one-pixel signals so that results obtained by these experiments can be taken as lower limits of the respective impact. I.e. in reality, and for larger non-rain echo areas, the impacts are expected to be more pronounced than what results from these experiments.

A large number of of experiments, i.e. 125, have been conducted, varying the clutter intensity I_f = 2, 5, 10, 20, 30, 50, 60 mm/h, the forcing times t_f from 2 min up to 2 hours. The varying degree of instability with the boundary layer moisture content results in differing lifting condensation levels and levels of free convection. Often, these levels are lower for environments of larger instabilities.

r_{max} (g/kg)	CAPE (J/kg)	LCL (m)	LFC (m)
10	400	1630	2840
11	800	1450	2400
12	1200	1290	2040
13	1700	1130	1730
14	2200	990	1470

Table 1: Specifications of the environments used for the numerical experiments. Values include the maximum water vapour mixing ratio in the boundary layer, CAPE, lifting condensation level and level of free convection.

3 Results

3.1 Description of a single experiment

Figure 1b,c) summarises the outcome of two individual experiments both conducted in a 1700 J/kg CAPE atmosphere, with a 10 mm/h clutter forced during 20 min (solid lines in panel b) and 6 min (dashed line). The model response to the applied forcing is depicted in terms of maximum up- and downdraft (panel b) and total accumulated precipitation (panel c). The larger forcing causes an updraft which reaches a strength of 1 m/s after about 7 min. Continuing the forcing out to 20 min does not increase the vertical velocity, but keeps it at this level even though a slight modulation is visible, indicating an interaction between the forcing and the developing model dynamics. However, after having switched off the forcing air parcels seem to have reached the level of free convection sometime between 20 and 30 min. Once this level is reached the instability present in the basic state is released, exhibiting values of the vertical velocity up to 13 m/s at t = 52 min. Substantial rain falls out beginning at t = 41 min. and stops when the system relaxes at t = 60 min. Total rainfall accumulates close to $0.1 \cdot 10^6$ m^3 whereas the precipitation equivalent of the forcing amounts to $0.01 \cdot 10^6$ m^3, i.e. the error given by the non-rain echo has been amplified by the assimilation

scheme by a factor of close to 10. Note, that in this experiment downdrafts form of several m/s in response to the convectively driven updraft.

The second experiment in Fig. 1b,c), on the other hand, is an example in which the initial erroneous forcing is not sufficient to lift air parcels to their level of free convection. Hence the initially triggered vertical velocity gradually decreases without producing any precipitation and downdrafts.

3.2 Evaluation of the idealised clutter experiments

The impact of a particular non-rain echo on the assimilation and the subsequent forecast in an individual experiment can be measured as the ratio of the resulting model-produced precipitation *R_mod* and the precipitation equivalent of the total forcing *R_f* calculated from the product of the forcing time *t_f* and the clutter amplitude *I_f* (Fig. 1c). If the ratio *R_mod*/*R_f* is zero or much smaller than one, the effect of the spurious signal on the assimilation is negligible. If, however, the ratio is larger than one, the assimilation has amplified the error in the radar data. In the former case, the conditional instability present in the environment was not released by the applied forcing, i.e. it is too small to lift an air parcel to reach the level of free convection. For the latter, however, this level is eventually reached and the instability released. Consequently, the model-produced rain can be much larger than the forcing equivalent. The instability is accompanied by significant values of vertical velocity of the order of several tens of m/s as illustrated in Fig. 1b).

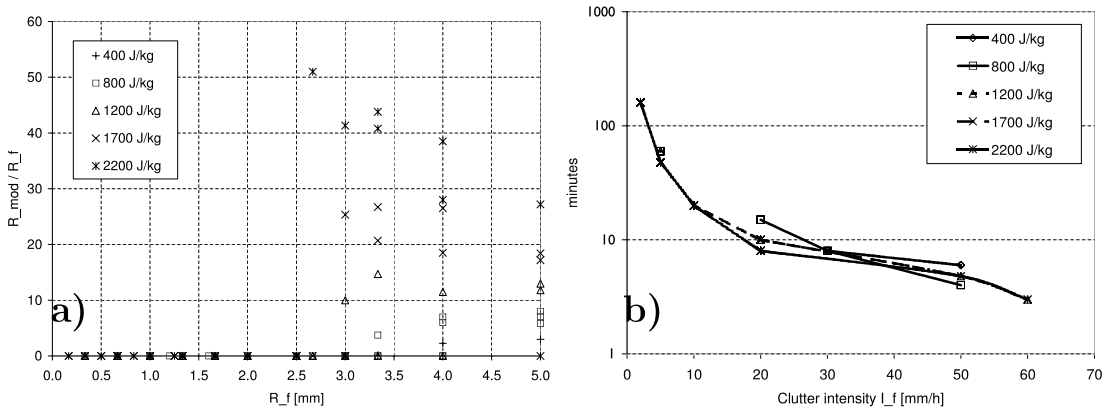

Figure 2: Panel a): Sensitivity of the Latent Heat Nudging scheme to ground clutter-like non-rain echoes (refer to Section 3.2). The symbols denote individual experiments in which a single-pixel forcing was applied during various periods of time in atmospheres of various instabilities. The x-axis denotes the total applied forcing (i.e. the product of intensity of the echo times the time over which it is applied), the y-axis the ratio of the resulting total model precipitation and the total forcing. Note, that even for relatively moderate instabilities amplification of the signal (i.e. ratio larger than 1) takes place after modest forcing. Panel b): Minimum time needed for the Latent Heat Nudging scheme to amplify a ground clutter-like non-rain echo for various instabilities (denoted by different symbols (refer to Section 3.2). The x-axis represents the clutter amplitude (mm/h), while the y-axis the critical forcing time (min) in logarithmic scale. Note, that for the higher clutter amplitudes it takes only a few minutes of forcing for the amplification to take place.

The ensemble of one-pixel clutter experiments with zero wind is evaluated in terms of the

resulting amplification factors which are summarised in Fig. 2a). It becomes evident that even medium-intensity ground clutter signals can be dramatically amplified in unstable environments and, therefore, hamper the precipitation assimilation substantially. This occurs when the forcing induced by the spurious echo is sufficient to lift air parcels to their level of free convection. For instance, a clutter signal of 20 mm/h nudged during 10 min into an environment with a CAPE of 1200 J/kg, is amplified by a factor of 15, while in a 400 J/kg environment a 50 mm/h clutter amplifies by a factor of 3 after 8 minutes, i.e. even for relatively moderate instabilities amplification of the signal (ratio larger than 1) takes place after modest total forcing. Accompanying updrafts easily reach values between 10 and 20 m/s. This scatter plot suggests the existence of a threshold forcing, for the present configuration at R_f between 2.5 and 3 mm, above which air parcels do reach their level of free convection, and the instability is released. However, there are cases with a larger total forcing, e.g. 10 mm resulting from a combination of small clutter intensity and long forcing time, in which the level of free convection is not attained. This may partly be due to an interference of the LHN forcing with the model dynamics (such as numerical diffusion), when the convective system starts to develop in the model. Investigation of this is beyond the scope of the present study.

A slightly different way of representation is given in Fig. 2b), in which the critical forcing time t_crit, i.e. the minimum time for a given amplitude to reach amplification, is depicted for several degrees of instability. Again, for unstable environments even very small amplitude signals are amplified given sufficient forcing time. For high-amplitude signals dramatic error amplification is almost immediate, i.e. takes place after as little as a few minutes. For smaller values of CAPE and clutter amplitude, however, the assimilation scheme is able to dampen the error.

In the light of these results and given that real ground clutter amplitudes often reach, or even exceed, such amplitudes, a thorough clutter elimination in convectively unstable situations seems to be fundamental.

3.3 Real case example

In order to illustrate what can happen in real cases of clutter, Swiss Radar Network (SRN) data for a non-rain day are assimilated for a six hour period into the experimental setup of this study using the reference profile with CAPE=800 J/kg (Fig. 1a). The simulation was performed with the setting used by LR05, i.e. a model domain of 361×333 horizontal grid points, with a mesh size of 2.2 km and 45 vertical levels. The six hour accumulation of the resulting model precipitation (Fig. 3b) exhibits dramatic amplification of the original clutter signals. It is evident that regions of large coherent clutter amplify to larger intensities than pixel-sized signals, as the former are less dampened by the model's numerical diffusion scheme that acts primarily on the structures with sizes of the order of the gridlength. The problem is somewhat mitigated if the SRN data are run through a Shapiro type observation filter with length 4 (Shapiro 1975) (Fig. 3c). In addition, the presence of appreciable wind causes the precipitation resulting from the clutter assimilation to be exported to neighbouring regions, in which new convection can be triggered (Fig. 3d).

3.4 Anomalous propagation conditions

The signal resulting from anomalous propagation of the radar beam is another important source of non-rain echoes (e.g. Koistinen et al., 2004). In contrast to regular ground clutter, anomalous propagation clutter can be more coherent in space but more intermittent in time.

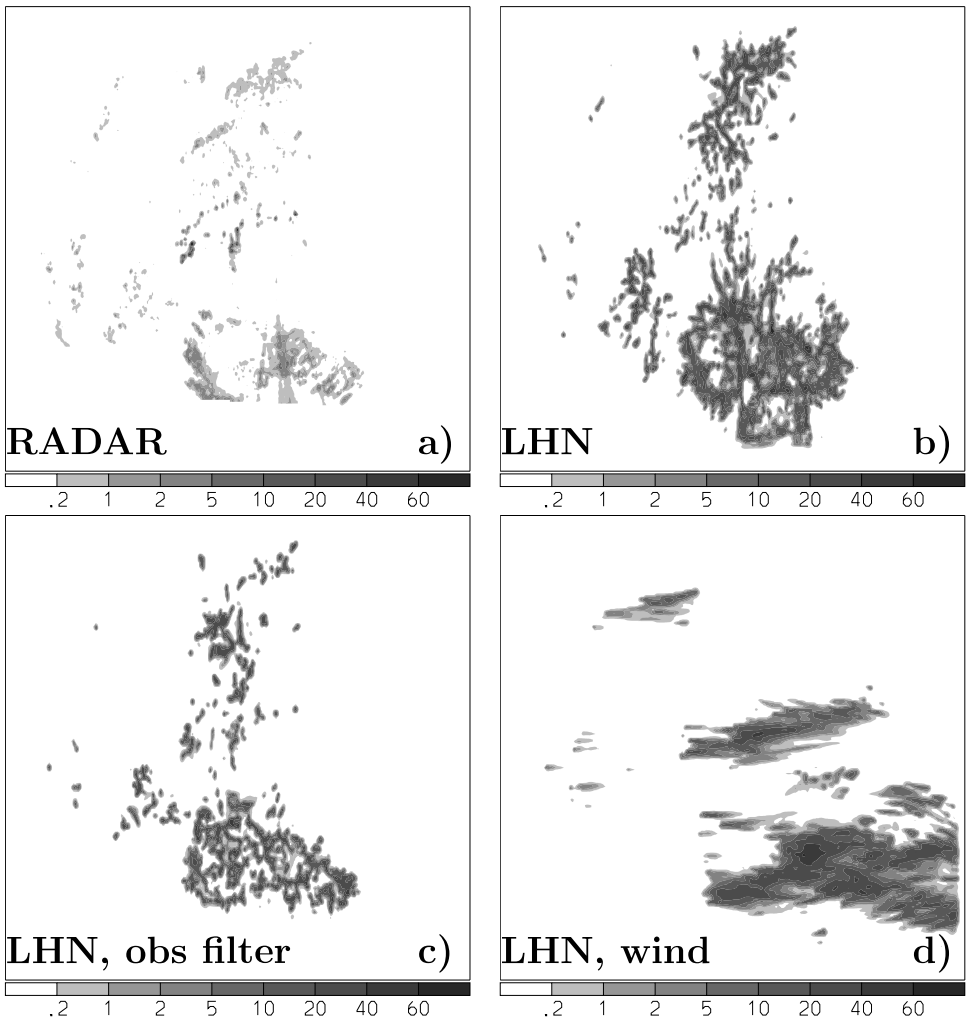

Figure 3: Examples for the assimilation of real clutter in a convectively unstable situation. Panel a) shows a six-hour accumulation (mm/h) of the Swiss Radar Network for a non-rain day, and panel b) displays the model precipitation resulting from a continuous forcing of the clutter by LHN. Panel c) is as b) except that the observed clutter is filtered. Finally, panel d) is as b) except that wind is added in the basic state. The domain has a size of $730 \times 800\,\mathrm{km}$.

In Switzerland, conditions conducive to anomalous propagation are characterized by very stable conditions and often occur in concomittance with low-stratus, in which often very dry upper-level air tops the planetary boundary layer and the thermal inversion, thus giving rise to strong vertical refractivity gradients. Consequently, assimilating such clutter signals does not usually result in precipitation amplification, due to the absence of convective instability and sufficient moisture. However, the LHN forces the model in trying to match the model precipitation with the input signal. As the model does not produce precipitation the forcing is continued and may yield significant vertical circulations throughout the troposphere. Values for up-downdrafts can reach $7\,\mathrm{m/s}$ and $-2\,\mathrm{m/s}$, respectively (Fig. 4a). This spurious circulation may distort the dynamical fields locally and interact adversely with the mesoscale flow. In particular, substantial vertical mixing of the local model atmosphere can take place. Fig. 4b) illustrates how more humid air of the boundary layer is generously mixed into the dryer air of the free troposphere. This effect would be undesired, for instance, in the context of air pollution modelling, as critical pollution episodes are usually tied to strong inversions. However, this issue was not pursued further in this study.

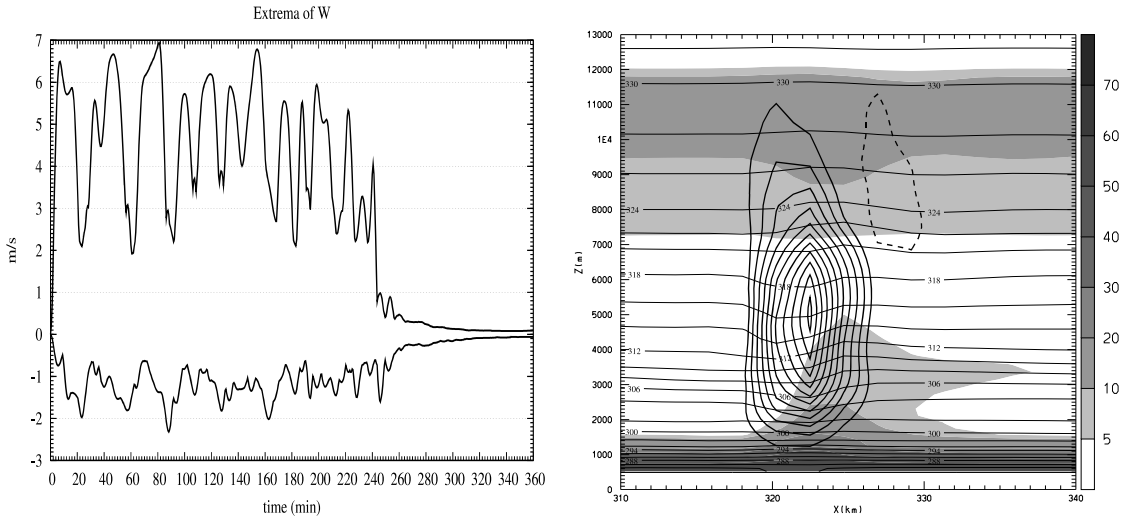

Figure 4: Panel a): Time evolution of the maximum up- and downdraft (m/s) during the assimilation experiment in conditions conducive to anomalous propagation of the radar beam. Positive values denote updrafts, negative values downdrafts. The forcing is applied during 4 hours. Panel b): Vertical cross-section through maximum updraft of the anaprop experiment at 2h into simulation time. Displayed are RH (in %, shaded), potential temperature (2K contour interval, thin lines) and vertical velocity (0.5 m/s contour interval, bold lines, solid updrafts, dashed downdrafts).

4 Summary and discussion

In this study the sensitivity of the Latent Heat Nudging (LHN) scheme to non-rain echoes was investigated by means of idealised experimentation with synthetic and real radar data. It constitutes one part of an effort to judge the LHN's aptness as an efficient and economic scheme for operational high-resolution rainfall assimilation. The main findings of this study are:

- non-rain, or clutter, echoes as small as one pixel can trigger the release of convective instabilities when forced by the LHN scheme;
- the resulting precipitation can be large compared to the original signal, i.e. factors 3 up to 50 have been found for moderate to high value of CAPE;
- the response of the model atmosphere to the forcing is very quick, i.e. on the time scale of convection (less than ten minutes for strong forcing to a couple of hours for moderate forcing);
- large, coherent areas of non-rain echoes pose a more stringent problem;
- filtering the input data can significantly mitigate the problem;
- non-rain echoes resulting from anomalous propagation of the radar beam in a low-stratus case over Switzerland, by virtue of the usually stable and dry conditions associated, are not conducive to error amplification. However, a strong spurious vertical circulation, along with undesired mixing, may be induced and adversely impact the mesoscale circulation.

A limitation of the study is that the impact of non-rain echoes is investigated in isolation. The negative impact found may be less dramatic in situations, when clutter is embedded in

real precipitation echoes. Furthermore the LHN scheme used in this study does not contain the modifications of Klink and Stephan (2005), i.e. it is not compatible with the prognostic treatment of precipitation. However, given the highly idealised nature of the sensitivity experiments we expect the findings of this study to apply, at least qualitatively, also for the new version of the LHN scheme for the following reasons: Firstly the 1×1 clutter pixel is constant in time and space, secondly there is no horizontal wind in most of the experiments and thirdly the forcing time of the LHN scheme would not be much different if the vertically integrated precipitation flux would be taken as model reference precipitation.

Characterisation of the radar data quality for use in atmospheric data assimilation schemes is very important. It has been shown that errors can, in certain circumstances, be dramatically amplified and cause the QPF to deteriorate. Quality characterisation of radar data could, therefore, include at the pixel level some sort of probability for the signal to be rain in terms of a static clutter map of zero probability of rain and a dynamic estimate of varying amplitude. An assimilation scheme like LHN can include such information into a quality or weighting function as proposed by Jones and MacPherson (1977) and Leuenberger and Rossa (2003). It is conceivable to make the assimilation of pixels with non-zero probabilities for being spurious conditional on the prevailing atmospheric conditions. For instance, a pixel with a 50% probability of being real rain would be assimilated in stable to neutral environments, while rejected in highly unstable situations. The dialog between radar data producer and users is absolutely vital in this context.

References

Germann, U., and J. Joss, 2004: Operational measurement of precipitation in mountainous terrain. *Weather Radar. Principles and Advanced Applications*, P. Meischner, Ed., Springer Verlag, pp. 52–75.

Jones, C. D., and B. Macpherson, 1997: A latent heat nudging scheme for the assimilation of precipitation data into an operational mesoscale model. *Meteorol. Appl.*, 4, 269–277.

Klink, S., and K. Stephan, 2005: Latent heat nudging and prognostic precipitation, *COSMO Newsletter*, No. 5, available from http://www.cosmo-model.org.

Koistinen, J., D. B. Michelson, H. Hohti, and M. Peura, 2004: Operational measurement of precipitation in cold climates. *Weather Radar. Principles and Advanced Applications*, P. Meischner, Ed., Springer Verlag, pp. 78–114.

Leuenberger, D., 2005: High-resolution radar rainfall assimilation: Exploratory studies with latent heat nudging, Ph.D. thesis, Swiss Federal Institute of Technology, Zürich, Switzerland.

Leuenberger, D., and A. Rossa, 2003: Assimilation of radar information in aLMo, *COSMO Newsletter*, No. 3, available from http://www.cosmo-model.org.

Shapiro, R., 1975: Linear filtering. *Math. Comp.*, 29, 1094–1097.

Weisman, M. L., and J. B. Klemp, 1982: The dependence of numerically simulated convective storms on vertical wind shear and buoyancy. *Mon. Wea. Rev.*, 110, 504–520.